University of Reading

Mediterranean cyclones and windstorms in a changing climate

Article

Published Version

Creative Commons: Attribution 3.0 (CC-BY)

Open Access

Nissen, K. M., Leckebusch, G. C., Pinto, J. G. and Ulbrich, U. (2014) Mediterranean cyclones and windstorms in a changing climate. Regional Environmental Change, 14 (5). pp. 1873-1890. ISSN 1436-378X doi: 10.1007/s10113-012-0400-8 Available at https://centaur.reading.ac.uk/32732/

It is advisable to refer to the publisher's version if you intend to cite from the work. See Guidance on citing.

To link to this article DOI: http://dx.doi.org/10.1007/s10113-012-0400-8

Publisher: Springer

All outputs in CentAUR are protected by Intellectual Property Rights law, including copyright law. Copyright and IPR is retained by the creators or other copyright holders. Terms and conditions for use of this material are defined in the End User Agreement.

www.reading.ac.uk/centaur

CentAUR

Central Archive at the University of Reading

University of Reading

Reading's research outputs online

Reg Environ Change (2014) 14:1873–1890
DOI 10.1007/s10113-012-0400-8

ORIGINAL ARTICLE

Mediterranean cyclones and windstorms in a changing climate

Katrin M. Nissen · Gregor C. Leckebusch · Joaquim G. Pinto · Uwe Ulbrich

Received: 27 April 2012 / Accepted: 20 December 2012 / Published online: 19 January 2013
© The Author(s) 2013. This article is published with open access at Springerlink.com

Abstract Changes in the frequency and intensity of cyclones and associated windstorms affecting the Mediterranean region simulated under enhanced Greenhouse Gas forcing conditions are investigated. The analysis is based on 7 climate model integrations performed with two coupled global models (ECHAM5 MPIOM and INGV CMCC), comparing the end of the twentieth century and at least the first half of the twenty-first century. As one of the models has a considerably enhanced resolution of the atmosphere and the ocean, it is also investigated whether the climate change signals are influenced by the model resolution. While the higher resolved simulation is closer to reanalysis climatology, both in terms of cyclones and windstorm distributions, there is no evidence for an influence of the resolution on the sign of the climate change signal. All model simulations show a reduction in the total number of cyclones crossing the Mediterranean region under climate change conditions. Exceptions are Morocco and the Levant region, where the models predict an increase in the number of cyclones. The reduction is especially strong for intense cyclones in terms of their Laplacian of pressure. The influence of the simulated positive shift in the NAO Index on the cyclone decrease is restricted to the Western Mediterranean region, where it explains 10–50 % of the simulated trend, depending on the individual simulation. With respect to windstorms, decreases are simulated over most of the Mediterranean basin. This overall reduction is due to a decrease in the number of events associated with local cyclones, while the number of events associated with cyclones outside of the Mediterranean region slightly increases. These systems are, however, less intense in terms of their integrated severity over the Mediterranean area, as they mostly affect the fringes of the region. In spite of the general reduction in total numbers, several cyclones and windstorms of intensity unknown under current climate conditions are identified for the scenario simulations. For these events, no common trend exists in the individual simulations. Thus, they may rather be attributed to long-term (e.g. decadal) variability than to the Greenhouse Gas forcing. Nevertheless, the result indicates that high-impact weather systems will remain an important risk in the Mediterranean Basin.

Keywords Climate change · Mediterranean · Windstorms · Cyclones

K. M. Nissen (✉) · U. Ulbrich
Institute for Meteorology, Freie Universität Berlin,
Carl-Heinrich-Becker Weg 6-10, 12165 Berlin, Germany
e-mail: katrin.nissen@met.fu-berlin.de

G. C. Leckebusch
School of Geography, Earth and Environmental Sciences,
University of Birmingham, Edgbaston,
Birmingham B15 2TT, UK

J. G. Pinto
Institute for Geophysics and Meteorology,
University of Cologne, Kerpener Str. 13,
50937 Cologne, Germany

Introduction

The Mediterranean region (MR) has been recognised as one of the areas that will be strongly affected by climate change (e.g. Giorgi 2006). Among the natural hazards affecting this region, extreme cyclones play an important role: these high-impact weather events may cause windstorms, storm surges, landslides and flooding (De Zolt et al. 2006; Liberato et al. 2011; Lionello et al. 2010; Nissen et al. 2010). Thus, changes in cyclone occurrence

and characteristics are expected to play a main role in past, present and future changes of the MR climate. Here, we focus on cyclones and the occurrence of windstorms as one hazardous phenomenon related to cyclones.

Statistically significant negative trends in cyclone numbers affecting the MR have been detected for the recent past (e.g. Flocas et al. 2010; Maheras et al. 2001; Nissen et al. 2010; Trigo et al. 2000). On the other hand, while the number of explosive Mediterranean cyclones has possibly decreased, this reduction is not statistically significant (Kouroutzoglou et al. 2011a).

Research based on global climate model (GCM) simulations investigating Mediterranean cyclone activity under changing greenhouse gas (GHG) conditions has been summarised in the review paper by Ulbrich et al. (2009). For the MR, many GCM studies report a strong reduction in winter cyclone activity (Lionello et al. 2002; Geng and Sugi 2003; Pinto et al. 2006; Leckebusch et al. 2006; Bengtsson et al. 2006; Pinto et al. 2007; Löptien et al. 2008; Raible et al. 2010). With respect to cyclone intensity, the results are more controversial, as some models suggest a decrease in the frequency of the most intense systems (Pinto et al. 2007; Raible et al. 2010), while other models show more extreme events or an increase in the intensity of extreme cyclones (Lionello et al. 2002; Gaertner et al. 2007).

For extreme windstorms, Bengtsson et al. (2009) predict a reduction in the number of events exhibiting wind speeds above 35 m/s over the MR during winter at the end of the twenty-first century, under A1B conditions. They use the ECHAM5 model with a resolution of T213 (63 km) which shows a decrease in the 99.5 percentile of 925 hPa winds over the entire MR. For the ECHAM5 MPIOM model with T63 resolution, Pinto et al. (2007) found a significant decrease in the 98th percentile of the 10 m wind speed during the winter half year only for the southernmost parts of the MR, while no significant changes are present in the northern part. A simulation with the HadCM3 model with a resolution of 2.5° × 3.75° latitude/longitude produces a reduction in winds restricted to the eastern MR (Leckebusch and Ulbrich 2004).

The distribution and evolution of cyclones and windstorms in the MR for the ERA40 period has been analysed in Nissen et al. (2010). A technique to match the windstorms to the responsible cyclones was introduced. The approach demonstrated that considering the link between pressure and wind features helps to understand the mechanisms of windstorm variability. One particular result was the finding that a considerable number of windstorms in the MR is associated with cyclones on a track completely outside the MR. These systems typically pass over Western Europe towards the North and Baltic seas. As suggested by previous studies, such cyclones are likely to be affected in a different way by climate change than the cyclones located inside the MR (e.g. Pinto et al. 2007, 2009). In this study, we apply the same technique and investigate possible future changes in windstorms, local Mediterranean cyclones and non-local cyclones associated with Mediterranean windstorms. The role of the NAO on present day variability and future changes is examined. The analysis evaluates a total of 7 global coupled model experiments performed using two different model configurations. All simulations are based on the same model for the atmosphere, but one simulation is especially designed for Mediterranean systems as it was conducted with a higher spatial resolution than other previously available AOGCM simulations. The question is addressed, whether the simulated signals depend on the model resolution, which might be the case in the MR which is characterised by small-scale features in orography and ocean–land contrast.

The next section describes the model simulations used for the present study and the methods employed for the analysis. The model simulations are validated against observations in section "Simulation of the present day climate" and the climate change signal is analysed in section "Climate change signal". Links with the NAO are discussed in section "Links to NAO". Section "Summary and discussion" summarises the results.

Data and methods

Data

The study is based on coupled GCM simulations, which all use the ECHAM5 model (e.g., Roeckner et al. 2006) as their atmospheric component. Results from two different configurations are analysed: INGV CMCC and ECHAM5 MPIOM. In both configurations, the ECHAM5 model is integrated with 31 hybrid sigma-pressure levels in the vertical and the highest vertical level at 10 hPa.

In the ECHAM5 MPIOM configuration, the atmospheric horizontal resolution is T63 (corresponding to 1.875° × 1.875°). The ocean model MPIOM (e.g., Jungclaus et al. 2006) comprises 40 vertical levels and is run at a horizontal resolution of 1.5° × 1.5°.

The INGV CMCC model (e.g., Scoccimarro et al. 2011) uses a higher horizontal resolution for the atmosphere (T159 corresponding to 0.75° × 0.75°). The INGV CMCC system includes two ocean models. The global ocean component OPA8.2 (Madec et al. 1998) is run with 31 vertical levels and a horizontal resolution of approx. 2° × 2°. It uses a grid refinement in the equatorial region (0.5°). In addition, the system includes a Mediterranean Ocean model based on OPA9.0 with a horizontal resolution of 1/16° and 72 vertical levels. Due to the high horizontal

resolution and the use of a Mediterranean Ocean model, the INGV CMCC system is especially suitable for Mediterranean applications, as it is expected to provide a more realistic representation of the local ocean atmosphere feedbacks (like latent heat release) that are important for cyclone development (Chang et al. 1984). The disadvantage of this setup is the relatively high amount of computing time needed to run the model, limiting the number of years available for the analysis.

In total, we have analysed 7 model simulations. An ensemble of 3 ECHAM5 MPIOM simulations was forced with historical (20C) and SRES A1B scenario greenhouse gas concentrations. Another ECHAM5 MPIOM ensemble with 3 members was forced using the SRES A2 greenhouse gas concentrations. Both ensembles end in the year 2100. For the INGV CMCC model, only one simulation has been available, covering the period from 1950 to 2050, forced with historical and A1B greenhouse gas concentrations.

To validate the simulations, the results for the end of the twentieth century are compared to the results obtained using the ERA40 reanalysis data set (Uppala et al. 2005), which has a horizontal resolution of 1.125° × 1.125° and covers the period 1957–2002.

Methods

As both cyclone and windstorm activity are strongest during winter, the study is limited to the winter half year (October–March).

Cyclones are identified and tracked using an algorithm developed by Murray and Simmonds (1991a), Simmonds et al. (1999), which has been modified for Northern Hemisphere conditions by Pinto et al. (2005). The algorithm detects maxima in the Laplacian of pressure using the Mean Sea Level pressure field at 6 hourly intervals. For the tracking, the location and strength of the cyclone centre is predicted for the subsequent time step, and the most likely cyclone centre is then chosen as the next track element. Only systems existing over at least 24 h are kept. The number of cyclones detected and their Laplacian of pressure depend on the horizontal resolution of the data set (e.g. Pinto et al. 2005; Kouroutzoglou et al. 2011b). In order to obtain comparable cyclone climatologies, previous studies have identified sets of thresholds for the rejection of spurious depressions and cyclone tracks suitable for specific horizontal data resolutions. To allow comparison with existing publications, we adopt these thresholds. They were selected in order to have an optimal representation of the cyclone activity within and near the Mediterranean Basin, while keeping a good representation of the cyclone activity over the North Atlantic. For the ECHAM5 MPIOM simulations we use the same values as Pinto et al. (2007), which are summarised in Pinto et al. (2005). For the ERA40 reanalysis, the thresholds reported in Nissen et al. (2010) are used. A consistent adjustment was chosen for the much higher resolved INGV CMCC simulations. The minimum $\nabla^2 p$ values for open, closed and strong systems are set to: cmnc1 = 0.3; cmnc2 = 0.4; cmncw = 0.8 and the devaluation threshold in the tracking for new systems is set to qmxnew = 0.9. cmnc1, cmnc2, cmnc3, cnmcw and qmxnew are the names of the parameters used in the algorithm to allow comparison with Pinto et al. (2005).

Windstorms affecting the MR have been identified following Leckebusch et al. (2008): Adjoining grid boxes with near surface (10 m) wind speeds exceeding the local 98th percentile form a cluster, which is located and tracked using a nearest neighbour approach. The 98th percentile is determined individually for each grid point in each simulation based on the extended winter season for the period 1960–1999. In order to ensure that only organised, spatially coherent wind events are kept, a spatial threshold is introduced to the wind cluster identification. In Nissen et al. (2010), this threshold was set to approx. 45,000 km^2. We have retained this threshold for the ERA40 and the INGV CMCC data sets. Due to the lower resolution of the ECHAM5 MPIOM simulation, the threshold for the minimum cluster size had to be increased to approx 130,000 km^2, corresponding to 3 affected grid boxes. We consider 3 grid boxes as the lowest threshold for the extend of an event, in order to reject unorganised, random exceedances of wind speed percentiles. The higher area threshold leads to a lower number of extreme wind tracks analysed for ECHAM5 MPIOM. Missing are small-scale systems with relatively low integrated severity.

The intensity of a windstorm was investigated using the Storm Severity Index (SSI) developed by Leckebusch et al. (2008). The index takes the anomaly of the local wind speed, the affected area and the duration of the windstorm into account. It is only different from zero when the wind speed exceeds the local 98th percentile in a number of adjoining grid boxes. For this Mediterranean application, only grid boxes within the area 10°W–40°E 30°N–46°N contribute to the SSI. Strong (or large-scale) wind events affecting only the fringes of the MR will thus tend to have a smaller SSI value than weaker (or smaller) events affecting the Central MR.

The cyclone responsible for the windstorm was identified by matching the wind event to the most likely cyclone. The matching is based on the distance between the cyclone track and the wind track. If more than one cyclone track is found within a search radius of 800 km, the strongest system in terms of the Laplacian of pressure is chosen. The algorithm is described in detail in Nissen et al. (2010).

Changes of extreme events both in terms of cyclones and windstorms are quantified by evaluating changes in the distribution. This is performed by fitting a Generalised

Pareto Distribution (GPD) to the events set above a chosen threshold ("peak over threshold" method). Following Della-Marta and Pinto (2009), the GPD is fitted using the Maximum-Likelihood method. Uncertainty is calculated using the Delta method (cf. Coles 2001; Della-Marta et al. 2009). Return periods are significantly different (5 % level) between two distributions if the 83.4 % confidence interval of that return period does not overlap (Julious 2004). We applied this technique to the 6 ECHAM5 OM1 ensemble simulations which cover the complete twenty-first century and focus on events with a 5-year return period as a representative example for rare events.

Simulation of the present day climate

Cyclones

The cyclone track density (following Murray and Simmonds 1991b) for the extended winter season (October–March) for the period 1971–2000 shows generally a good agreement between the model simulations and the ERA40 reanalysis (Fig. 1a–c). All data sets feature the main cyclone path over the North Atlantic and a secondary maximum over the MR. The local maxima over the Golf of Genoa, Cyprus and the Black Sea are captured. The maximum over the Golf of Genoa in the ECHAM5 MPIOM is less pronounced than in the reanalysis and the INGV CMCC model, both in terms of the individual runs as well as the ensemble mean. This is apparently related to the comparatively low horizontal model resolution of ECHAM5 MPIOM (cf. section "Data"). The influence of the horizontal resolution on cyclones is known to be especially prominent in secondary storm track areas such as the MR but affects mostly weak and small-scale systems (Pinto et al. 2005; Trigo 2006; Jung et al. 2006; Kouroutzoglou et al. 2011b). Compared to the reanalysis, both GCMs simulate more cyclones than observed over the Black and the Caspian Sea, a feature which was already present in the previous model version ECHAM4 (Pinto et al. 2006).

The average numbers of cyclone tracks per extended winter season over the entire MR (10°W–40°E 30°N–46°N) are summarised in Table 1. Using the chosen thresholds for the cyclone identification algorithm, the highest number of events is found for the INGV CMCC model. In ECHAM5 MPIOM, the underestimation of events over the Golf of Genoa is more than compensated by the overestimation of cyclones over the Eastern MR, resulting in a higher total number of cyclones in ECHAM5 MPIOM compared to ERA40. The intensity of each cyclone is determined considering the maximum Laplacian of pressure observed inside the MR. The increase in $\nabla^2 p$ with increasing horizontal resolution, as described in section "Methods" can be noticed: The percentage of events with high $\nabla^2 p$ in INGV CMCC is higher than in the ERA40 reanalysis and the ECHAM5 MPIOM simulation.

The majority of the cyclones generated by the model simulations, which cross the MR, is also generated within the MR (63 %). This is comparable to the ERA40 reanalysis data set [67 %, Nissen et al. (2010)]. With increasing intensity (i.e. max $\nabla^2 p$ inside the MR), the share of cyclones originating inside the MR decreases. For the strongest 1 % of the events, only between 30 and 50 % are generated inside the MR, thus, up to 70 % enter the region from the outside (Fig. 2a). In this context, the most important area of cyclogenesis outside the MR is the North Atlantic region. Of the strongest 1 % (0.1 %) of the cyclones crossing the MR, 10–20 % (20–40 %) of the systems originate over this area (Fig. 2b).

The geographical distribution of the mean Laplacian of pressure agrees well between the reanalysis and the model simulations (Fig. 1d–f. All data sets show the highest Mediterranean values over Italy. The shift towards higher values of $\nabla^2 p$ with increasing resolution is also visible.

Windstorms

The spatial distribution of extreme wind tracks for the last 30 years of the twentieth century for the North Atlantic and European sector exhibits three main areas of extreme wind activity, which are located over the North Atlantic, Northern Europe and the MR (Fig. 3). For the MR, the ERA40 observations show the highest windstorm activity west of Italy, at the eastern coast of the Iberian Peninsula, the Ionian Sea and South of Cyprus. These areas are well captured by all model integrations considered. The lower number of windstorms in the ECHAM5 MPIOM ensemble is caused by a lack of small-scale events. This is a consequence of the coarser horizontal resolution, as the GCM wind events must cover a minimum number of grid boxes to be considered for further analysis (see explanation in section "Methods").

Cyclones associated with windstorms

By matching the windstorms to the responsible cyclones according to Nissen et al. (2010), it is possible to study the characteristics of cyclones leading to windstorms in the MR. Using the chosen thresholds, we detect an average of 46 windstorms per winter season affecting the MR in the ERA40 reanalysis data set, which can be associated with cyclones. In comparison, we identify 50 (32) extreme wind events associated with cyclones in the INGV CMCC (ECHAM5 MPIOM) simulations under present day climate

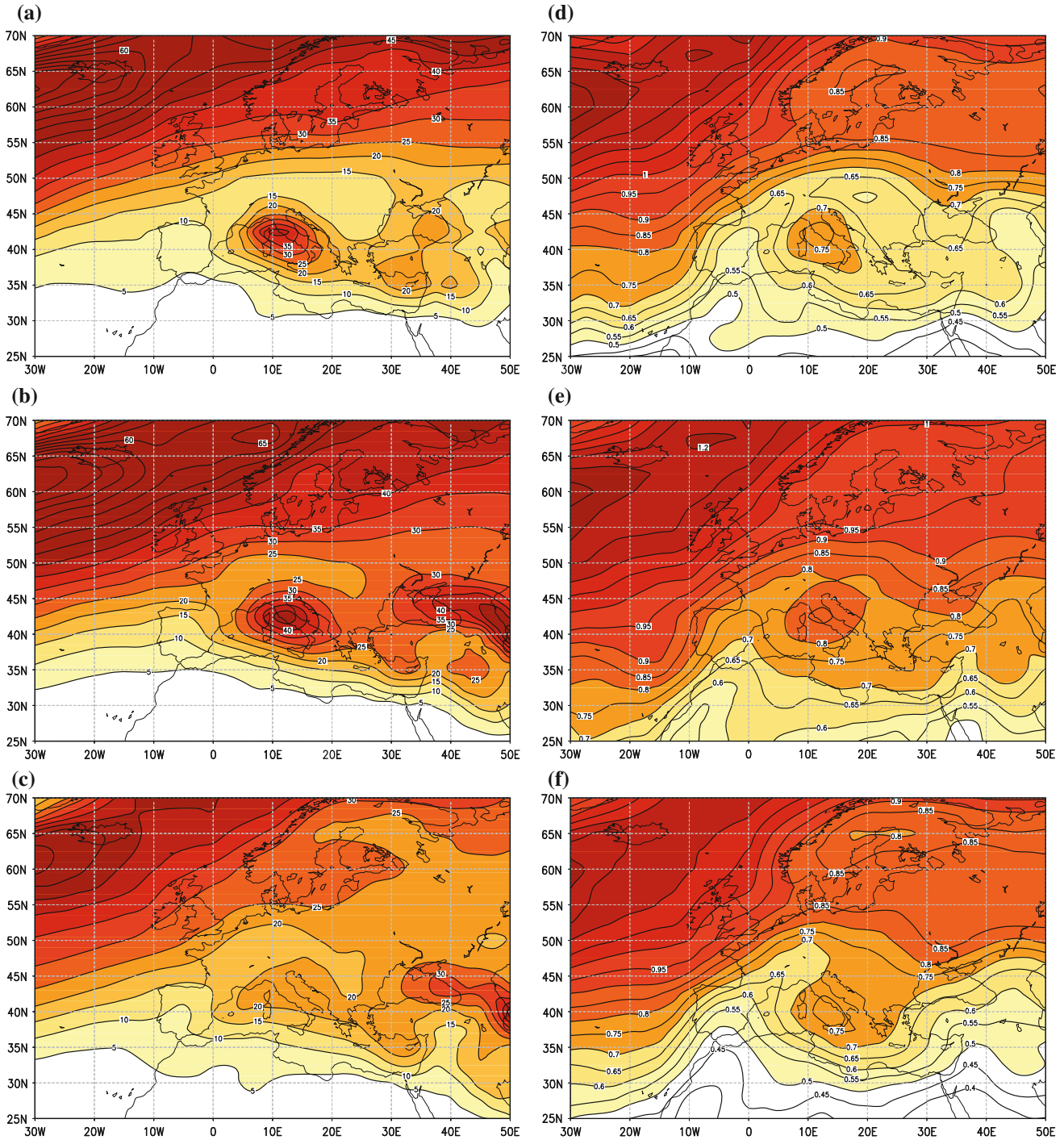

Fig. 1 *Left column* Cyclone track density for the extended winter season (October–March) for the period 1971–2000 **a** ERA40, **b** INGV CMCC simulation, **c** ECHAM5 MPIOM ensemble. In cyclone days per extended winter per (deg.lat.)^2. *Right column* Mean distribution of the Laplacian of pressure during the extended winter season in (deg.lat.)^2 for **d** ERA0, **e** INGV CMCC and **f** ECHAM5 MPIOM ensemble

conditions. In all data sets, approximately 8 % of the identified windstorms cannot be matched unambiguously to a cyclone. The majority of these unmatched events concerns wind tracks caused by two consecutive cyclones. They individually last less than 18 h and would have been rejected by the windstorm identification algorithm if they had not been joined together during the tracking procedure (Nissen et al. 2010).

For all data sets, the majority of the windstorms is associated with cyclones which themself cross the MR

Table 1 Cyclone track counts in the MR (10°W–40°E, 30°N–46°N) for the period 1971–2000 in numbers per year

	Total	$\nabla^2 p > 1.0$	$\nabla^2 p > 1.5$	$\nabla^2 p > 2.0$
ERA40	96	35 (36 %)	5 (5 %)	0.5 (0.5 %)
INGV CMCC	127	62 (49 %)	11 (9 %)	1.2 (1 %)
ECHAM5 ensemble	105	32 (30 %)	7 (7 %)	0.7 (0.7 %)

$\nabla^2 p$ refers to the maximum observed in the MR. Values in parentheses give % of the total amount

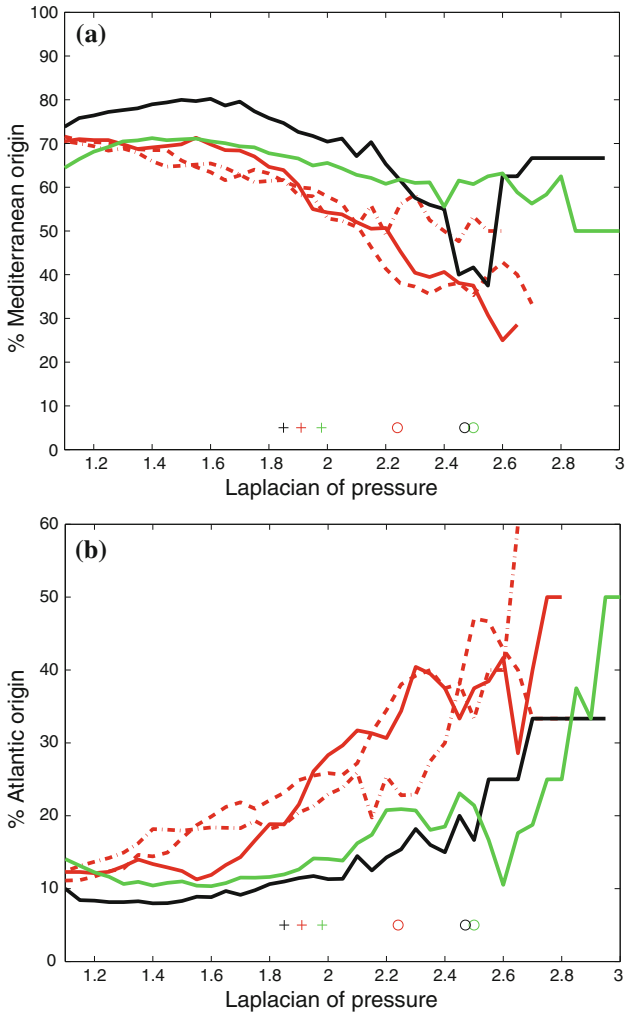

Fig. 2 Percentage of cyclones originating over **a** the MR or **b** the North Atlantic and later cross the MR. Dependence on cyclone intensity in terms of $\nabla^2 p$. Period 1971–2000. *Black* ERA40; *Red* ECHAM5 MPIOM simulations (*solid* ensemble member 1, *dashed* ensemble member 2, *dash dotted* ensemble member 3); *Green* INGV CMCC simulation. The coloured crosses denote the 90th and the *circles* the 99th percentile of $\nabla^2 p$ reached inside the MR (colour figure online)

(approx. 65 %). Windstorms caused by local cyclones typically affect a larger area inside the MR than windstorms associated with cyclones passing outside the MR, which often only affect its fringes. In addition, the average duration of a windstorm inside the MR is higher if the event is caused by a local cyclone (32 h instead of 19 h). As a result of those two effects, the SSI tends to be higher for local cyclones, because the affected areas outside the MR are not considered for the calculation of the SSI in this regional study. For the strongest 1 % of wind events, only about 10 % of the responsible cyclones never enter the MR, compared to 35 % when considering all events.

In ERA40 and the INGV CMCC model, about 60 % of the cyclones responsible for windstorms within the MR originate outside of the MR, mostly over the Atlantic Ocean (over 30 %), Northern Europe (over 10 %) and Northern Africa (between 5 and 10 %). The contribution of windstorm causing cyclones originating over the North Atlantic for the ECHAM5 MPIOM ensemble is about 10 % higher than in the reanalysis, while the contribution of systems originating in the MR is approximately 10 % lower (Table 2). With increasing windstorm severity, the share of wind causing cyclones originating inside the MR increases in the observations and all GCM experiments (not shown).

Windstorm causing cyclones, which cross the MR exhibits on average higher values of $\nabla^2 p$ than cyclones, which are not associated with extreme wind tracks (Table 3). In addition, their core pressure tends to be lower. Cyclones of Atlantic origin are typically more intense, both in terms of $\nabla^2 p$ and core pressure, than cyclones originating over the MR and are in relative terms more often associated with windstorms affecting the MR than cyclones of local origin. The percentage of identified cyclones which are responsible for windstorms and cross the MR is lower in the GCM than in ERA40.

Climate change signal

Cyclone frequency

In order to estimate the climate change signal, the differences between cyclone track densities for the extended winter season simulated under present day climate conditions and track densities anticipated for climate change conditions are determined (Figs. 4, 5). The panels in Fig. 4 show the differences between the periods 2021–2050 and 1971–2000 for the INGV CMCC integration forced with the A1B greenhouse gas scenario (Fig. 4a), the ECHAM5 MPIOM ensemble mean forced with the A1B greenhouse gas scenario (Fig. 4b) and the ECHAM5 MPIOM ensemble mean forced with the A2 greenhouse gas scenario (Fig. 4c), while Fig. 5 shows the differences between the end of the twenty-first century (2071–2100) and the period 1971–2000

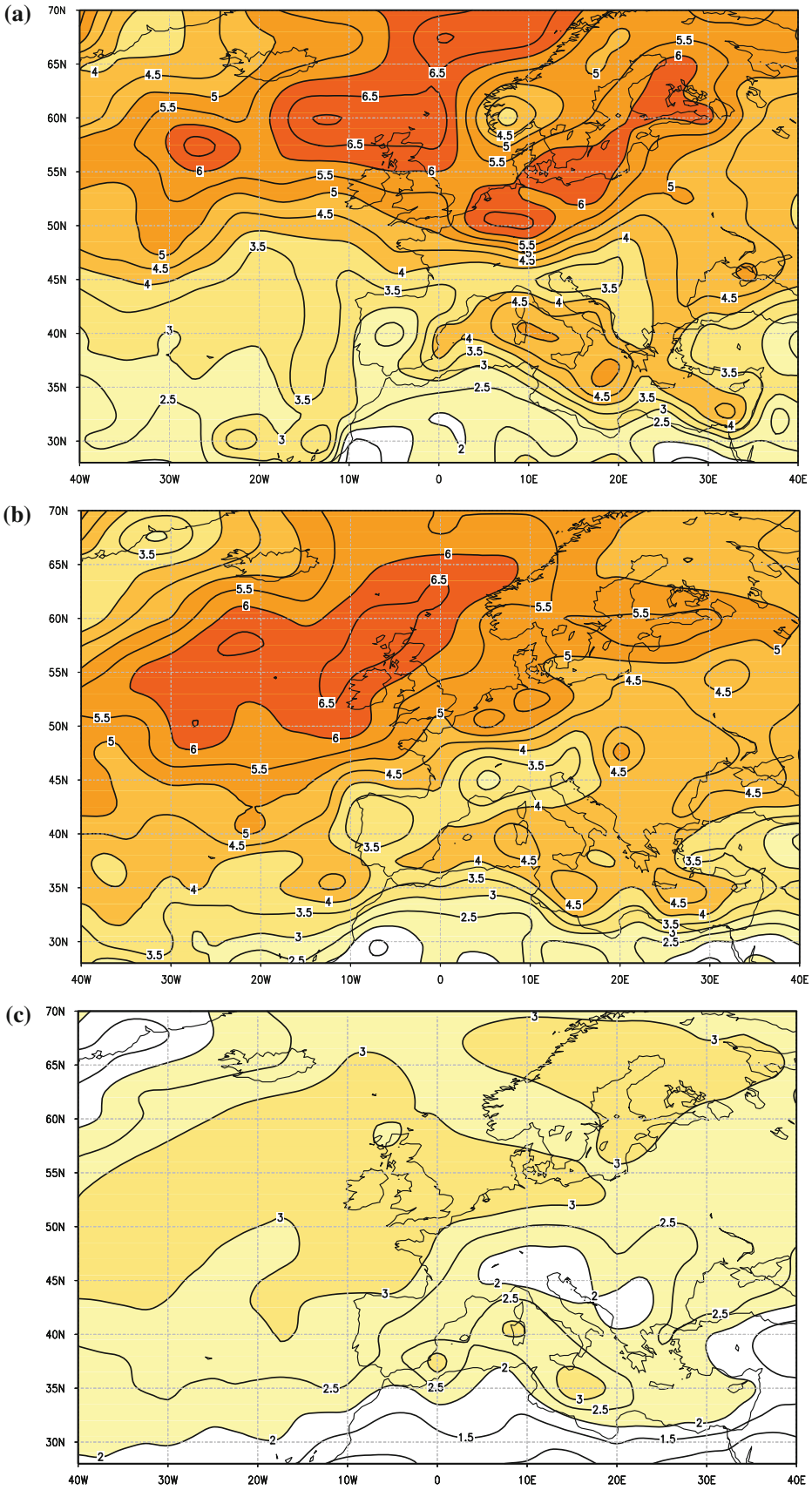

Fig. 3 Wind track density for the extended winter season (October–March) for the period 1971–2000 **a** ERA40, **b** INGV CMCC simulation, **c** ECHAM5 MPIOM ensemble. In windstorm days per extended winter per (deg.lat.)^2

Table 2 Area of genesis for cyclones causing windstorm in the MR

	ERA40	INGV CMCC	ECHAM5 MPIOM 1	ECHAM5 MPIOM 2	ECHAM5 MPIOM 3
Mediterranean (10°W–40°E/30°N–46°N)	584 (43 %)	549 (38 %)	349 (36 %)	304 (32 %)	319 (33 %)
Atlantic (<10°W)	435 (32 %)	496 (35 %)	401 (42 %)	434 (45 %)	415 (43 %)
Northern Europe (10°W–40°E/ >46°N)	162 (12 %)	199 (14 %)	123 (13 %)	141 (15 %)	118 (12 %)
Northern Africa (10°W–40°E/<30°N)	134 (10 %)	114 (8 %)	61 (6 %)	52 (5 %)	71 (7 %)
East of MR (>40°E)	48 (4 %)	71 (5 %)	25 (3 %)	24 (3 %)	34 (4 %)
Total	1,363	1,429	959	955	957

Table 3 Characteristics of windstorm causing and non-windstorm causing cyclones, which cross the MR

		ERA40	INGV CMCC	ECHAM5 MPIOM
MR	Share	27 % (73 %)	22 % (78 %)	15 % (85 %)
MR	$\nabla^2 p$	1.2 (1.0)	1.4 (1.2)	1.4 (1.0)
MR	p	998 (1,003)	995 (1,000)	994 (1,002)
Atl	Share	40 % (60 %)	37 % (63 %)	31 % (69 %)
Atl	$\nabla^2 p$	1.6 (1.3)	1.8 (1.4)	1.7 (1.2)
Atl	p	985 (989)	980 (989)	984 (995)
NE	Share	27 % (73 %)	25 % (75 %)	33 % (77 %)
NE	$\nabla^2 p$	1.3 (1.0)	1.5 (1.3)	1.5 (1.1)
NE	p	993 (999)	992 (996)	990 (1,000)

For cyclones originating over the Mediterranean (MR), over the Atlantic (Atl) and over Northern Europe (NE) (see Table 2 for area definitions). Values for non-windstorm causing cyclones are put in parenthesis. Compared are share in %, maximum of $\nabla^2 p$ along the track in hPa/(deg.lat.)^2 and minimum core pressure (p) in hPa. Based on the extended winter season 1971–2000

for the two ECHAM5 MPIOM ensembles. All analysed simulations show a statistically significant reduction in the number of cyclones over most of the MR. The relative reduction increases with cyclone strength in terms of the Laplacian of pressure, up to 2.4 hPa/(deg.lat)^2 (Fig. 6), which is consistent with the results reported by Pinto et al. (2007). A statistically significant increase in the total number of cyclones can only be found over the Levant region and to a limited extend over Morocco (Figs. 4, 5).

The ECHAM5 MPIOM simulations suggest that the reduction in cyclone frequency continues with increasing GHG forcing (Figs. 5, 6). The signal is present in all individual simulations (not shown) and the ensemble mean. The strongest reduction under both A1B and A2 forcing for the twenty-first century is located over the Ionian Sea (Fig. 5). The strongest decrease is simulated during the second half of the twenty-first century for the A2 scenario. After the first 50 years, the ensemble mean reduction in the number of cyclones over the Ionian sea for A2 is one system per winter season. After 100 years, the decrease has intensified to 6.5 systems per winter season. For both scenarios, cyclones generated outside and inside the MR are equally affected by the decrease (not shown).

Most intense cyclones

Cyclones with intensities above 2.0 $\nabla^2 p$ are rare events within the MR and occur on average only once every second year. In contrast to the changes for the cyclones of lower intensity, which occur multiple times per year, the reduction in the number of these events eventually becomes statistically non-significant and in some simulations even of opposite sign (Fig. 6). Note that the A1B ensemble indicates a positive trend for events with $\nabla^2 p > 2.6$ hPa/(deg.lat.)^2 during the first half of the twenty-first century and a negative trend during the second half of the century, in spite of the increasing GHG forcing. In addition, the sign of the signal in the 3 individual A1B simulations is not coherent (not shown).

The spatial distribution of these events suggests that the majority of the most extreme cyclones originates outside the MR (60 %). An historical and pertinent example of such an extreme system is the recent cyclone "Klaus" (23–24 January 2009), which propagated from the Bay of Biscay towards the Western Mediterranean and induced a strong storm surge (Liberato et al. 2011; Bertotti et al. 2012).

In line with previous work (e.g. Pinto et al. 2009), the highest intensities are reached over the Bay of Biscay and the Northern MR (not shown). One might argue that the Bay of Biscay should not be considered a Mediterranean region. Thus, the analysis has been repeated excluding the cyclones located over this area. It was found that this approach does not alter the results qualitatively.

In order to quantify possible changes in the frequency of the most intense cyclones, extreme value statistics is applied (cf. section "Data and methods"). As an representative example, we focus here on events with an intensity (Laplacian of pressure) correspondent to a 5-year return period during the historical period 20C (1961–2000). The analysis includes all cyclones which pass the MR, but excludes systems, which only pass over the Bay of Biscay. The 5-year return value for the ensemble is 2.16 hPa/(deg.lat.)^2. Using this fixed value as a threshold, the return periods are estimated for 40-year windows, which start in 1961, and are moved forward in time in 1-year intervals.

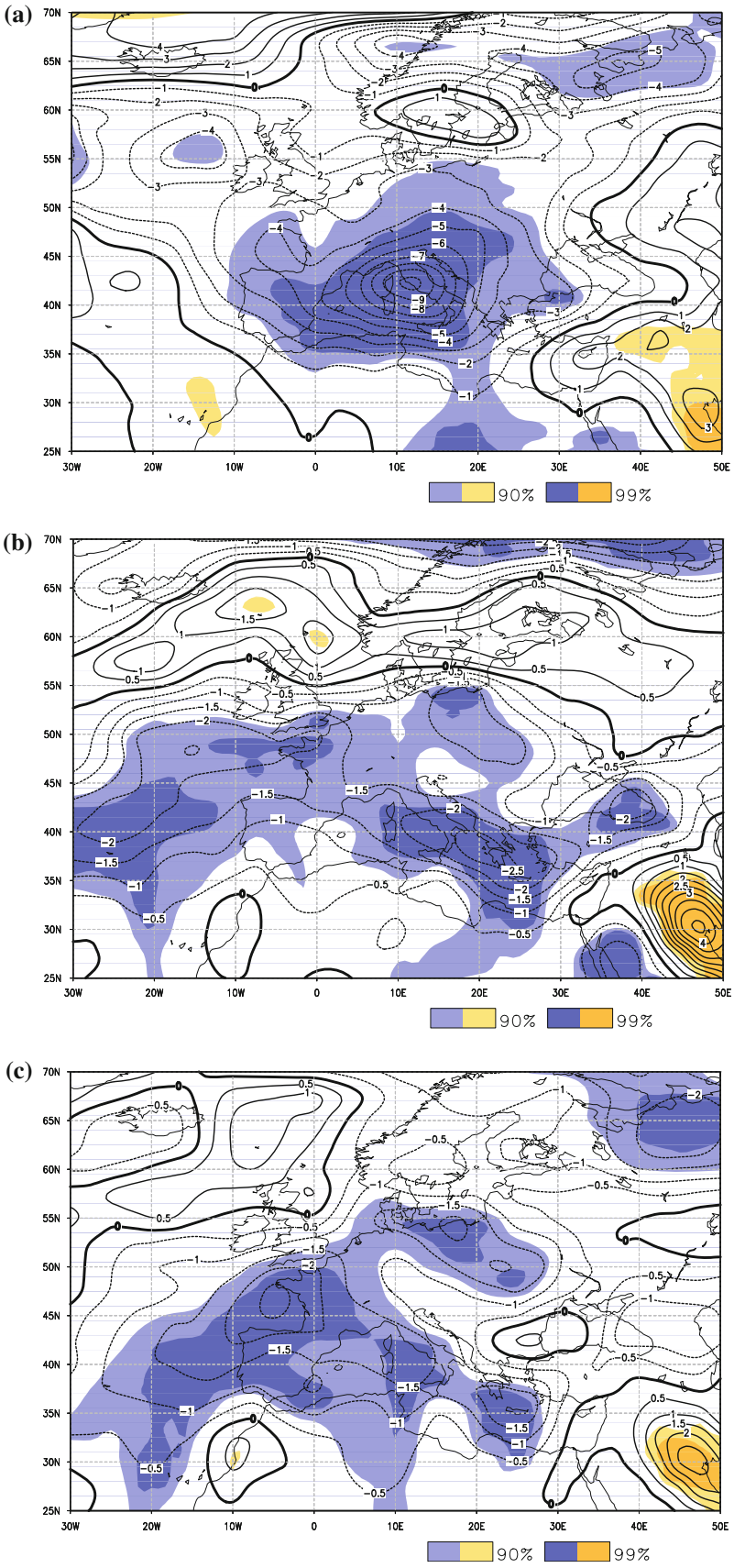

Fig. 4 Changes in cyclone track density for the extended winter season (October–March). Difference between the periods 2021–2050 and 1971–2000 **a** INGV CMCC simulation, **b** ECHAM5 MPIOM ensemble A1B scenario, **c** ECHAM5 MPIOM ensemble A2 scenario. In cyclone days per extended winter per (deg.lat.)^2

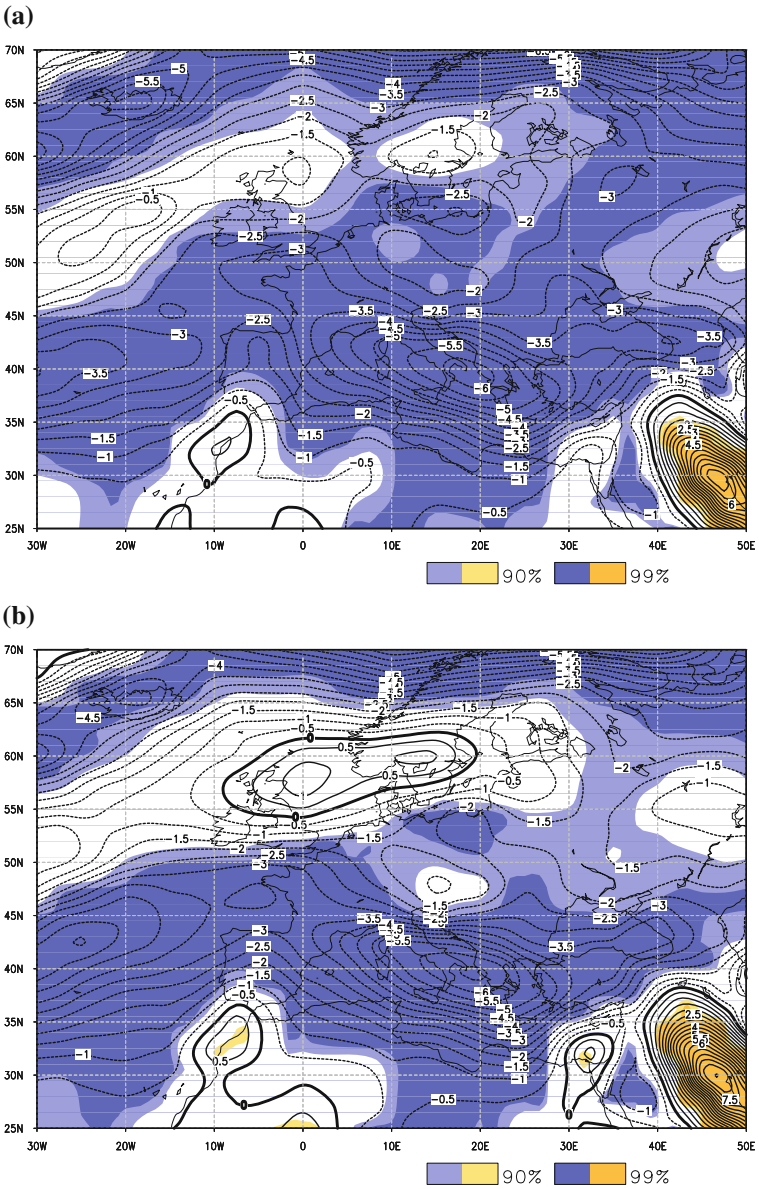

Fig. 5 Changes in cyclone track density for the extended winter season (October–March). Difference between the periods 2071–2000 and 1971–2000 **a** ECHAM5 MPIOM ensemble A1B scenario, **b** ECHAM5 MPIOM ensemble A2 scenario. In cyclone days per extended winter per $(\text{deg.lat.})^2$

The return period (blue line) and the corresponding 83.4 % confidence intervals (red lines) are calculated for each 40-year time window (Fig. 7). As stated in section "Simulation of the present day climate", the changes are significant (on the 95 % level) if the 83.4 % confidence interval estimated for the climate change period leaves the confidence interval determined for the 20C period (dotted lines).

For both scenarios, the ensemble mean exhibits typically shorter return periods (more frequent events) during the scenario period than for the end of the twentieth century, when considering these rare, most intense cyclones. However, statistically significant differences in the A1B ensemble can be only found between 2020 and 2045 (shaded area). For the A2 ensemble, a statistically significant reduction in the return period is reached close to the end of the simulation period. It should be noted that the individual runs in both ensembles exhibit considerable variability in the return frequency of the most intense Mediterranean cyclones and no clear common trend can be found (not shown).

This indicates that while the total number of cyclones decreases, the frequency of rare events shows considerable long-term variability. Therefore, systems with a higher intensity than under current climate conditions may be identified.

Windstorm frequency

All model simulations (individual runs and ensemble mean) predict a decrease in the number of extreme wind

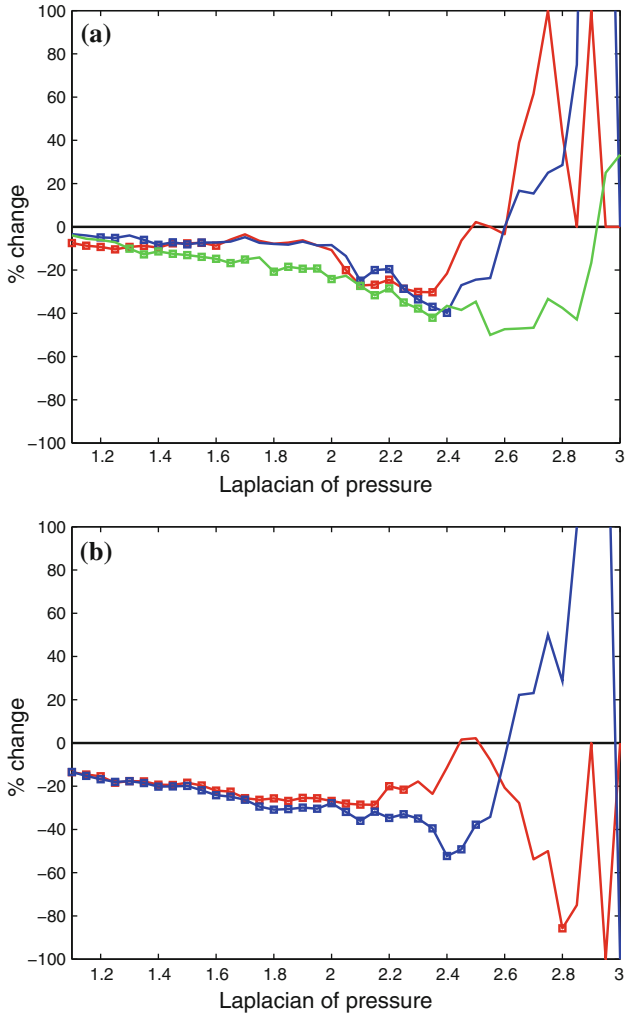

Fig. 6 Change in the number of cyclones crossing the MR compared to the period 1971–2000 in per cent. Dependence on cyclone strength in terms of $\nabla^2 p$ for overlapping intensity ranges of $\nabla^2 p = 0.5$. **a** Difference to period 2021–2050; **b** Difference to period 2071–2100. *Red* ECHAM5 MPIOM ensemble A1B forcing; *Blue* ECHAM5 MPIOM ensemble A2 forcing; *Green* INGV CMCC simulation. Markers (*rectangles*) denote statistically significant changes on the 95 % level (colour figure online)

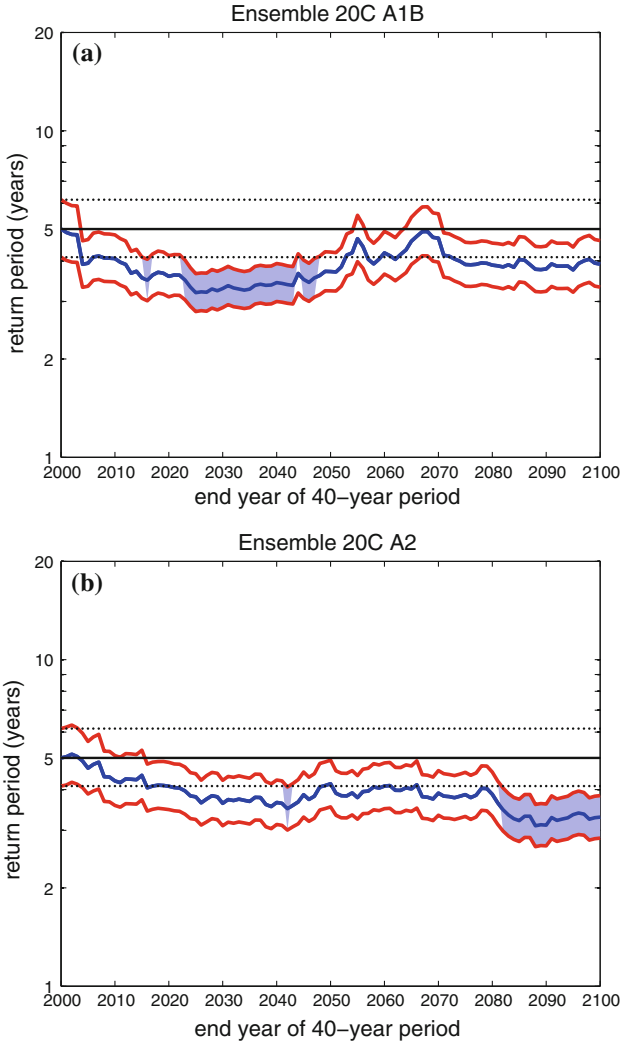

Fig. 7 5-year return period for extreme Mediterranean cyclones ($\nabla^2 = 2.16$, which is the 5-year return value for the period 1961–2000 in the ECHAM5 MPIOM ensemble). Calculated using a moving 40-year window. For **a**) ECHAM5 MPIOM ensemble A1B scenario **b**) ECHAM5 MPIOM ensemble A2 scenario. The *red lines* and the *broken lines* denote the 83 % confidence intervals. *Shading marks* periods with statistical significant changes on the 95 % level (colour figure online)

tracks over most of the MR (Fig. 8). In the INGV CMCC model, this reduction is statistically significant over the Central and Southern MR. In the ECHAM5 MPIOM ensembles, statistical significance is restricted to the southernmost parts of the MR. With increasing GHG, forcing the reduction continues and becomes statistically significant over a wider area (Fig. 9). The highest percental reduction with respect to 20C numbers is simulated for A2 GHG forcing during the second half of the twenty-first century.

All models predict a statistically significant increase in the number of extreme wind tracks over North Western Europe. This is in line with the results by Pinto et al. (2009), which identified a significant increase in the number of extreme cyclones over the British Isles and North Sea area, inducing a significant shortening in the return periods of such events over this area (Della-Marta and Pinto 2009). The affected area extends in some locations southward into the Northern MR. The exact location of the anomalies varies between the model configurations. In the ECHAM5 MPIOM ensembles, the Balkan region experiences an increase in the number of wind storms, which becomes statistically significant for the longer simulations. The INGV CMCC model on the other hand predicts a decrease in the number of wind events for the Balkan region but an increase (not statistically significant) over the northern part of the Iberian Peninsula.

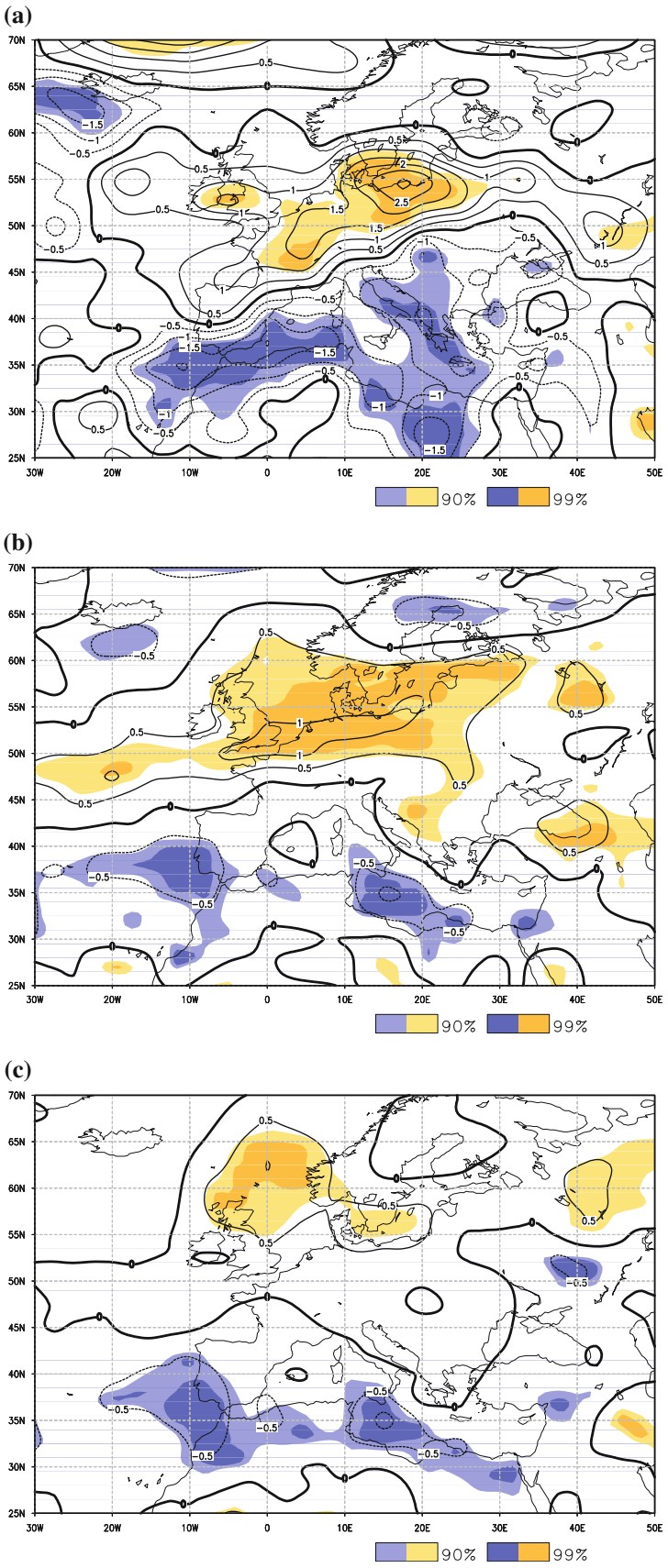

Fig. 8 Changes in wind track density for the extended winter season (October–March). Difference between the periods 2021–2050 and 1971–2000 **a**) INGV CMCC simulation **b**) ECHAM5 MPIOM ensemble A1B scenario **c**) ECHAM5 MPIOM ensemble A2 scenario. In windstorm days per extended winter per (deg.lat.)^2

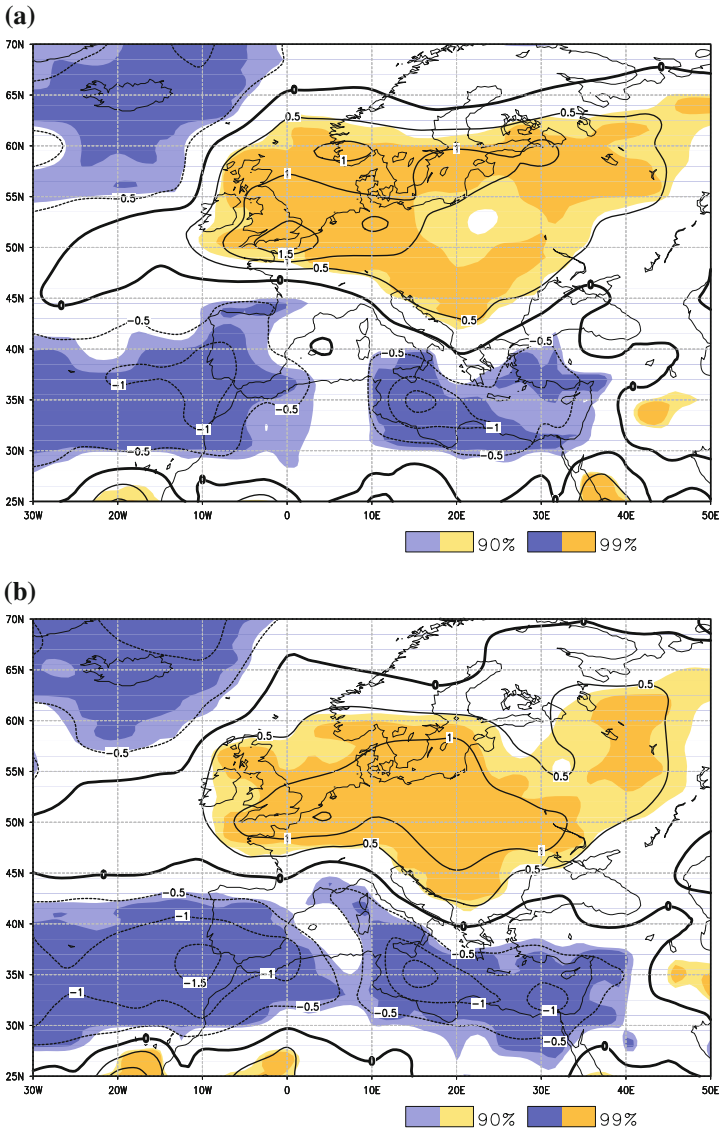

Fig. 9 Changes in wind track density for the extended winter season (October–March). Difference between the periods 2071–2100 and 1971–2000 **a**) ECHAM5 MPIOM ensemble A1B scenario **b**) ECHAM5 MPIOM ensemble A2 scenario. In windstorm days per extended winter per (deg.lat.)^2

While the number of windstorms associated with cyclones which never enter the MR slightly increases, the number of events associated with cyclones which cross the MR decreases. Wind events associated with cyclones generated inside the MR and events caused by cyclones first detected outside the MR, which later cross the region, decrease at equal rates. The overall result is the decrease in the number of wind events affecting the MR.

Windstorm intensity

Analogue to the approach described in section "Most intense cyclones", extreme value statistics is used to estimate possible changes in the return period of the most severe wind storms. As a reference value, the 5-year return value in 20C (1961–2000) has been estimated using the Mediterranean SSI values occurring during the extended winter season. It corresponds to a value of 5.9, which is approximately the 99.9th percentile in 20C. The A1B ensemble shows a decrease in the SSI 5-year return period during the first half of the twenty-first century (higher windstorm activity) (Fig. 10a). The return period returns to 20C levels at the end of the twenty-first century. In contrast to this, the A2 ensemble starts with a period of lower windstorm intensity but then shows a steady reduction in the return periods until the end of the century (Fig. 10b). For both scenarios, the changes in the return period never become significant above the 99 % value (not shown). Statistical significance on the 95 % level is reached in the A1B scenario around the year 2030 (shaded area). There is no clear common trend in the individual ensemble members. In addition, the signal does not appear to have a link

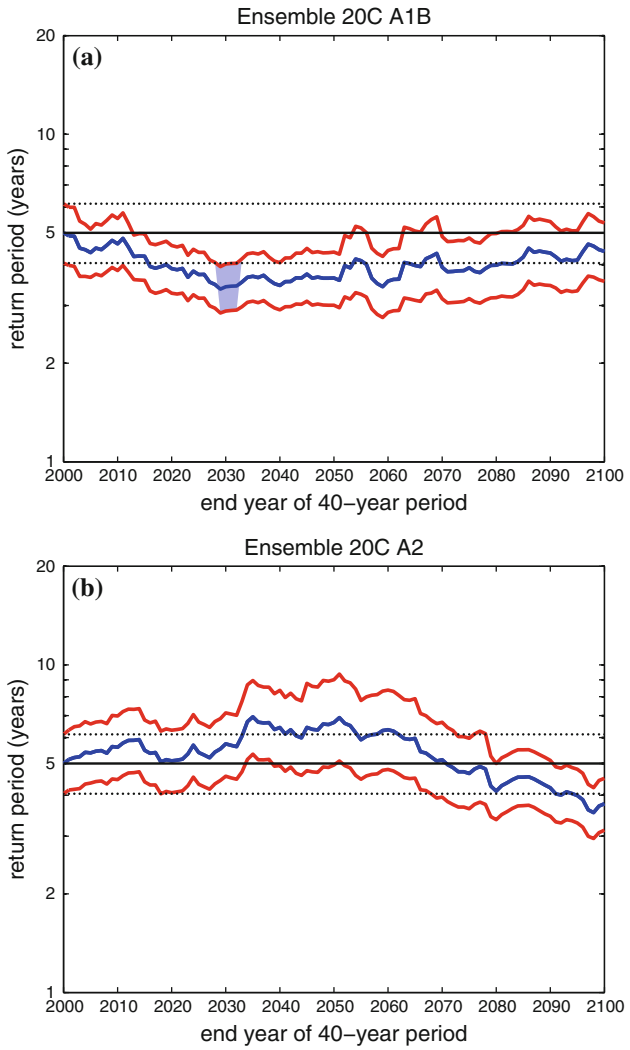

Fig. 10 5-year return period for extreme Mediterranean windstorms (SSI = 5.9, which is the 5-year return value for the period 1961–2000 in the ECHAM5 MPIOM ensemble). Calculated using a moving 40-year window. For **a** ECHAM5 MPIOM ensemble A1B scenario, **b** ECHAM5 MPIOM ensemble A2 scenario. The *red lines* and the *broken lines* denote the 83 % confidence intervals. *Shading marks* periods with statistical significant changes on the 95 % level (colour figure online)

with the increasing GHG forcing, and thus, the projected changes over time are most likely caused by long-term (e.g. decadal) variability and/or sampling effects.

The fact that the analysis of the ECHAM5 simulations does not provide evidence of a clear change in the return period of the most severe windstorms, even though the total number of windstorms affecting the MR decreases, can probably be attributed to a small number of extraordinary windstorms. In fact, events with a magnitude unseen under current climate conditions are identified during twenty-first century period. In the 6 ECHAM5 MPIOM ensemble simulations, of the 11 most severe events, 10 occur during the scenario period. In the INGV CMCC simulation, 3 windstorms are detected during the scenario period which exceed the maximum storm strength found during 20C. Such assessment agrees with results by Pinto et al. (2012), which showed for the ECHAM5 MPIOM simulations that the magnitude of the top ranking events may considerably increase even if the return periods do not change significantly (see their section 5.4.). They attribute this to the fact that changes on the magnitude of top ranking events are naturally more sensitive to single events, while changes in return periods are less sensitive to such outliers, as the statistical GPD model is fitted on many more events.

Figure 11 shows an example for an extreme windstorm occurring during the scenario period in an ECHAM5 MPIOM simulation (A1B forcing). A cyclone (red track) enters western Europe from the North Atlantic. The cyclone splits. One centre decays over western Europe and the other centre, which is first detected over the Golf of Lion, crosses Northern Italy and leaves the MR in north eastward direction. Its core pressure reaches a minimum of 943 hPa and the Laplacian of pressure goes up to a value of 2.6. The wind speed exceeds the local 98th percentile by more than 6 ms^{-1}. The event affects most of the MR. The Mediterranean SSI value of the event is 25.7. For comparison, the strongest event occurring during the twentieth century in the ECHAM5 MPIOM ensemble simulations has an SSI of 18.9, and the most severe event in the scenario period has an SSI of 48.8.

For the 5 most severe events (i.e. highest SSI), we have analysed the cyclone development in more detail. Of the 5 events, 3 enter the MR from the North Atlantic (this includes the case shown in Fig. 11). One cyclone develops close to the Iberian Peninsula and one cyclone is generated over Croatia. Four cyclones exhibit explosive deepening rates (the reference value at 45°N is 19.6 hPa/24 h, (c.f. Trigo 2006)), while the intensification of the remaining cyclone is slower (10 hPa/24 h). Baroclinicity at the time of the strongest cyclone deepening is analysed by calculating Eady growth rates (e.g. Hoskins and Valdes 1990). For 4 of the events, Eady Growth rates exceed the local 99th percentile (calculated for the extended winter season during the period 1961–2000) along the cyclone path prior to the phase of strongest cyclone intensification (green lines in Fig. 11). For the cyclone originating near the Iberian Peninsula, the maximum Eady growth rates found along the cyclone path only exceed the local 95th percentile. For this event, the cyclone intensification takes place over Romania and coincides with the occurrence of an upper level cut-off low. Upper level cut-off lows affecting the MR are mostly known for their potential to trigger extreme precipitation during summer (e.g. Gimeno et al. 2007). In Nissen et al. (2010), we also found a connection between upper level troughs and the development of extreme wind producing cyclones during the winter

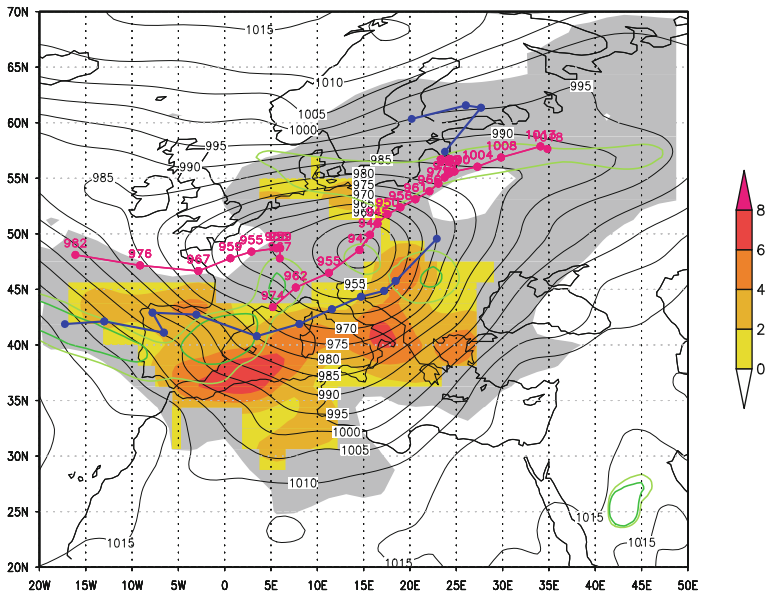

Fig. 11 Example for very severe windstorm. Cyclone track (*red*), wind cluster track (*blue*), mean sea level pressure field (*isolines*) and exceedance of 98th percentile of wind speed (*coloured shading*) for November 2070 in ECHAM5 MPIOM simulation forced with A1B greenhouse gas scenario. The total area with wind speeds exceeding the 98th percentile over the duration of the windstorm is shown in *grey*. The *green* contours indicate exceedance of the 95th and 99th percentile of local Eady growth rates at the day of the strongest cyclone intensification (colour figure online)

season over the Eastern MR using the ERA40 reanalysis data set. The relatively cold air from high latitudes in the cut-off lows can lead to instability and cyclone growth, an effect, which has also been observed in the lee of large-scale, upper-level blocking heights over the Northern Atlantic (Prezerakos et al. 1999). Such cold air intrusion often plays a role in the development of extreme cyclones in the MR and might have played a role in the formation of the exceptional windstorm event detected in the model.

Links to NAO

As expected from previous work (Nissen et al. 2010), more cyclones cross the MR during a negative NAO phase (approx. 20 %) compared to its positive phase (Fig. 12). This relationship is captured by all considered model experiments. The modulation in cyclone numbers is associated with a shift of the mean cyclone path, which is more southerly with negative NAO, than during its positive phase.

Additionally, Pinto et al. (2009) show that the NAO also influences cyclone growth factors over the North Atlantic. During the positive phase of the NAO, favourable conditions exist for cyclone intensification, resulting in a higher percentage of extreme cyclones over the North Atlantic. In order to test whether the NAO also influences growth conditions for Mediterranean cyclones, the ratio between extreme and non-extreme cyclones over the MR has been determined for different NAO phases. It was found that the phase of the NAO has no clear influence on the cyclone strength. This suggests that the NAO influences the number of cyclones crossing the MR but not necessarily their intensity.

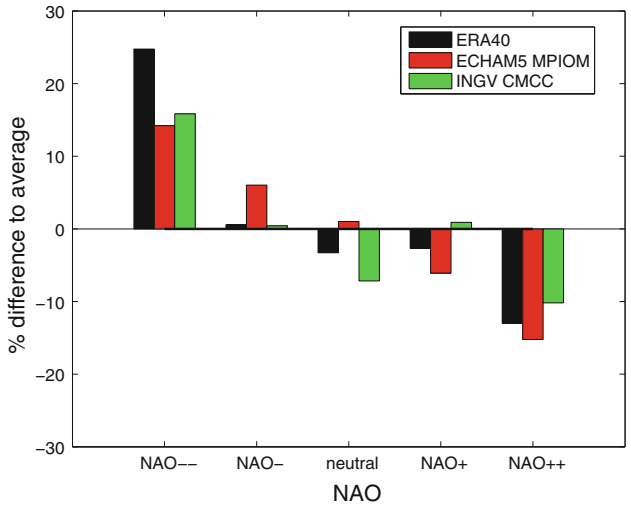

Fig. 12 Dependence of the number of cyclones crossing the MR on the phase and strength of the NAO based on the period 1971–2000. Expressed as percentage deviation from the average. The monthly mean NAO index has been determined using fixed grid points at Iceland and Portugal. NAO−− : index <-1.5; NAO−: $-1.5 \leq$ index < -0.5; neutral: $-0.5 \leq$ index < 0.5; NAO+: $0.5 \leq$ index < 1.5; NAO++: index ≥ 1.5. *Black* ERA40; *Red* ECHAM5 MPIOM ensemble simulations; *Green* INGV CMCC simulation

In all GCM simulations and the reanalysis data set, the number of windstorms affecting the MR is between 5 and 20 % higher during a strong negative NAO phase (i.e. NAO index <-1.5). This can be attributed to an increase in the number of windstorm producing cyclones originating over the North Atlantic and is in line with general increase in the number of cyclones during the negative phase of the NAO, which is in turn associated with a southerly shift of the preferred cyclone pathway (see above). The increase in wind producing cyclones with Atlantic origin during a

strong negative NAO phase is between 20 and 50 % compared to the average number of storm producing cyclones originating over this region. As a consequence, the risk of windstorms increases in the western MR during phases with negative NAO index.

The higher number of windstorms affecting the central MR during positive NAO phases, which was found in ERA40 (Nissen et al. 2010), is not captured by the low-resolution ECHAM5 MPIOM simulations. In the higher resolved INGV CMCC simulation, the signal is present, but less pronounced than in the observations (not shown).

Part of the cyclone decrease simulated under climate change conditions over most of the MR might be associated with the modelled shift of the NAO to a more positive index. The NAO index is increasing over the scenario period for the ECHAM5 MPIOM (see Pinto et al. 2007) and to a lesser extend in the CMCC model simulations (not shown). In order to make a rough estimate of the influence of the NAO on the simulated cyclone decrease, a linear regression analysis has been applied to the individual simulations on a monthly basis (not shown). The analysis shows the strongest influence of the NAO on the simulated cyclone trend for the western MR with a maximum in the region around the Golf of Lion. In this region, the NAO can explain between 10 and 50 % of the cyclone trend, depending on the individual simulation. In the region with the highest simulated cyclone trend over the Ionian sea, the influence of the NAO is neglectable for the model simulations.

Summary and discussion

In this paper, we have analysed the influence of GHG forcing on the frequency and intensity of cyclones and associated windstorms affecting the Mediterranean. The considered coupled GCM simulations all use the ECHAM5 model as their atmospheric component. One GCM configuration exhibits a considerably higher resolution in the atmosphere and the ocean and is used to analyse whether the simulated climate change signals depend on the model resolution.

The spatial distribution of cyclone track density in the MR in the higher resolved INGV CMCC simulation is closer to the ERA40 observations than in the lower resolved ECHAM5 MPIOM experiments. This agrees with the results of other authors. They found that the influence of the resolution is twofold: Both truncation and dynamical effects result in a reduction in detected systems when the horizontal model resolution is decreased (Jung et al. 2006). The effect is known to be particularly pronounced in secondary storm track areas such as the MR (Pinto et al. 2005). Most affected by a decrease in resolution are weak and small-scale systems preferentially in areas where cyclogenesis is associated with orography, for example, in the Golf of Genoa (Pinto et al. 2005; Trigo 2006; Kouroutzoglou et al. 2011b). The horizontal resolution also affects windstorms. Windstorms in ECHAM5 MPIOM have to be of greater spatial extend to be identified, resulting in a lower number of detected systems. Despite the differences in total numbers of detected wind and cyclone tracks and the differences in the local distribution, when considering the entire MR, the mean cyclone and windstorm characteristics are captured by both model configurations. In particular, the climate change signals are very similar in all simulations. This agrees with Trigo (2006), who compared cyclones detected in two reanalysis data sets. ERA40 at a resolution of 1.125° × 1.125° and NCEP/NCAR at 2.5° × 2.5° resolution exhibit similar trends in cyclone numbers, despite differences in the total number of identified systems and the local distribution.

In this study, we consider individual model runs and ensembles out of the available model experiments and distinguish between the climate change signals simulated for two different periods (2021–2050 and 2071–2100) characterised by different GHG levels. All simulations show a statistically significant reduction in the number of cyclones over most of the MR for the period covering the next decades, which is consistent with previous studies (e.g. Leckebusch et al. 2006; Bengtsson et al. 2006; Pinto et al. 2007; Löptien et al. 2008; Ulbrich et al. 2009; Raible et al. 2010). At the same time, a statistically significant increase in the number of cyclones is simulated over the Levant region, in line with results by Raible et al. (2010). The cyclone decrease is larger for the A2 scenario simulations, in line with the GHG forcing. The magnitude of the decrease depends on cyclone strength in terms of the Laplacian of pressure. Up to the 99th percentile of $\nabla^2 p$ the decrease is more pronounced for stronger cyclones. This relationship, however, does not apply to the most intense systems with return periods of several years. Due to the fact that the most intense cyclones within the simulation period are detected during the scenario period, the return frequency of the most extreme cyclones affecting the MR ($\nabla^2 p >$ 99.9th percentile) increases in the ECHAM5 MPIOM ensembles. These most intense systems mostly originate outside the MR and affect the Northern MR. There is no common trend in the individual simulations and no apparent connection to the underlying GHG forcing. We thus conclude that the occurrence of such systems probably has to be attributed to decadal variability and/or sampling effects.

The total number of windstorms affecting the MR is predicted to decrease over most of the area. In all simulations, the changes in the frequency of the windstorms between the end of the twentieth century and the first half of the twenty-first century are statistically significant over

the southern MR and in case of the INGV CMCC simulation over the Central MR. The decrease continues during the second half of the twenty-first century. The reduction in the number of windstorms can be attributed to a reduction in extreme wind producing cyclones crossing the MR. The number of Northern European cyclones (which never enter the MR) associated with windstorms in the MR slightly increases.

The most severe windstorms in terms of the SSI occur during the scenario period. A connection between the occurrence of the detected most extreme windstorms and the increase in greenhouse gas concentrations during the scenario period could not be established, as the simulations show partially disagreeing signals. As for the most intense cyclones, the occurrence of these most extreme windstorms might be due to decadal variability and/or sampling effects.

Although anthropogenic climate change may not be the direct cause for the simulated changes for the most extreme cyclones and windstorms, it is an important result of this study that their return period does not significantly change during the twenty-first century. Nevertheless, the most extreme cyclones and largest SSI values affecting the MR are identified during the scenario period, even though the total number of system decreases. This is in line with results by Pinto et al. (2012) using the 6 ECHAM5 MPI-OM simulations considered here. Thus, we conclude that high impact weather systems will remain an important risk in the Mediterranean Basin and that forecasting systems and civil protection will need to continue the ongoing development of strategies to issue early warnings due to extreme cyclones and windstorms.

Acknowledgments This work has been funded by the EU integrated project Climate Change and Impact Research: the Mediterranean Environment (CIRCE), project no. 036961. We would like to thank the two anonymous reviewers for their valuable suggestions, which helped to improve the manuscript.

Open Access This article is distributed under the terms of the Creative Commons Attribution License which permits any use, distribution, and reproduction in any medium, provided the original author(s) and the source are credited.

References

Bengtsson L, Hodges KI, Roeckner E (2006) Storm tracks and climate change. J Clim 19:3518–3543. doi:10.1175/JCLI3815.1

Bengtsson L, Hodges KI, Keenlyside N (2009) Will extratropical storms intensify in a warmer climate?. J Clim 22:2276–2301. doi:10.1175/2008JCLI2678.1

Bertotti L, Bidlot J, Bunney C, Cavaleri L, Delli Passeri L, Gomez M, Lefèvre J, Paccagnella T, Torrisi L, Valentini A, Vocino A (2012) Performance of different forecast systems in an exceptional storm in the Western Mediterranean Sea. Quart J Roy Meteorol Soc 138:34–55. doi:10.1002/qj.892

Chang CB, Pepkey DJ, Kreitzberg CW (1984) Latent heat induced energy transformations during cyclogenesis. Mon Weather Rev 112:357–367. doi:10.1175/1520-0493(1984)112<0357:LHIETD>2.0.CO;2

Coles S (2001) An introduction to modeling of extreme values. Springer, New York

De Zolt S, Lionello P, Nuhu A, Tomasin A (2006) The disastrous storm of 4 November 1966 on Italy. Nat Hazards Earth Syst Sci 6:861–879. doi:10.5194/nhess-6-861-2006

Della-Marta PM, Pinto JG (2009) Statistical uncertainty of changes in winter storms over the North Atlantic and Europe in an ensemble of transient climate simulations. Geophys Res Lett 36:L14703. doi:10.1029/2009GL038557

Della-Marta PM, Mathis H, Frei C, Liniger MA, Kleinn J, Appenzeller C (2009) The return period of wind storms over Europe. Int J Climatol 29:437–459. doi:10.1002/joc.1794

Flocas HA, Simmonds I, Kouroutzoglou J, Keay K, Hatzaki M, Bricolas V, Asimakopoulos D (2010) On cyclonic tracks over the eastern Mediterranean. J Clim 23:5243–5257. doi:10.1175/2010JCLI3426.1

Gaertner MA, Jacob D, Gil V, Domínguez M, Padorno E, Sánchez E, Castro M (2007) Tropical cyclones over the Mediterranean Sea in climate change simulations. Geophys Res Lett 34:L14711. doi:10.1029/2007GL029977

Geng Q, Sugi M (2003) Possible change of extratropical cyclone activity due to enhanced greenhouse gases and sulfate aerosols—study with a high-resolution AGCM. J Clim 16:2262–2274. doi:10.1175/1520-0442(2003)16<2262:PCOECA>2.0.CO;2

Gimeno L, Trigo RM, Ribera P, García JA (2007) Editorial: Special issue on cut-off low systems (COL). Meteorol Atmos Phys 96:1–2. doi:10.1007/s00703-006-0216-5

Giorgi F (2006) Climate change hot-spots. Geophys Res Lett 33:L08,707. doi:10.1029/2006GL025734

Hoskins BJ, Valdes PJ (1990) On the existence of storm-tracks. J Atmos Sci 47:1854–1864. doi:10.1175/1520-0469(1990)047<1854:OTEOST>2.0.CO;2

Julious AA (2004) Using confidence intervals around individual means to assess statistical significance between two means. Pharm Stat 3:217–222. doi:10.1002/pst.126

Jung T, Gulev SK, Rudeva I, Soloviov V (2006) Sensitivity of extratropical cyclone characteristics to horizontal resolution in the ECMWF model. Quart J Roy Meteorol Soc 132:1839–1857. doi:10.1256/qj.05.212

Jungclaus JH, Keenlyside N, Botzet M, Haak H, Luo JJ, Latif M, Marotzke J, Mikolajewicz U, Roeckner E (2006) Ocean circulation and tropical variability in the coupled model ECHAM5/MPI-OM. J Clim 19:3952–3972. doi:10.1175/JCLI3828.1

Kouroutzoglou J, Flocas HA, Keay K, Simmonds I, Hatzaki M (2011) Climatological aspects of explosive cyclones in the Mediterranean. Int J Climatol 31:1785–1802. doi:10.1002/joc.2203

Kouroutzoglou J, Flocas HA, Simmonds I, Keay K, Hatzaki M (2011) Assessing characteristics of Mediterranean explosive cyclones for different data resolution. Theor Appl Climatol 105:263–275. doi:10.1007/s00704-010-0390-8

Leckebusch GC, Ulbrich U (2004) On the relationship between cyclones and extreme windstorm events over Europe under climate change. Glob Planet Chang 44:181–193. doi:10.1016/j.gloplacha.2004.06.011

Leckebusch GC, Koffi B, Ulbrich U, Pinto JG, Spangehl T, Zacharias S (2006) Analysis of frequency and intensity of European winter storm events from a multi-model perspective, at synoptic and regional scales. Clim Res 31:59–74. doi:10.3354/cr031059

Leckebusch GC, Renggli D, Ulbrich U (2008) Development and application of an objective storm severity measure for the

northeast Atlantic region. Meteor Z 17:575–587. doi:10.1127/0941-2948/2008/0323

Liberato MLR, Pinto JG, Trigo IF, Trigo RM (2011) Klaus—an exceptional winter storm over northern Iberia and southern France. Weather 66:330–334. doi:10.1002/wea.755

Lionello P, Dalan F, Elvini E (2002) Cyclones in the Mediterranean region: the present and the doubled CO2 climate scenarios. Clim Res 22:147–159. doi:10.3354/cr022147

Lionello P, Cavaleri L, Nissen KM, Pino C, Raicich F, Ulbrich U (2010) Severe marine storms in the Northern Adriatic: characteristics and trends. Phys Chem Earth 40:93–105. doi:10.1016/j.pce.2010.10.002

Löptien U, Zolina O, Gulev S, Latif M, Soloviov V (2008) Cyclone life cycle characteristics over the Northern Hemisphere in coupled GCMs. Clim Dyn 31:507–532. doi:10.1007/s00382-007-0355-5

Madec G, Delecluse P, Imbard M, Lévy C (1998) OPA8.1 Ocean general circulation model reference manual. Note du Pole de modélisation, Institute Pierre-Simon Laplace, 11:91pp

Maheras P, Flocas HA, Patrikas I, Anagnostopoulou C (2001) A 40 year objective climatology of surface cyclones in the Mediterranean region: spatial and temporal distribution. Int J Climatol 109–130. doi:10.1002/joc.599

Murray RJ, Simmonds I (1991) A numerical scheme for tracking cyclone centres from digital data. Part I: development and operation of the scheme. Aust Meteorol Mag 39:155–166

Murray RJ, Simmonds I (1991) A numerical scheme for tracking cyclone centres from digital data. Part II: application to January and July general circulation model simulations. Aust Meteorol Mag 39:167–180

Nissen KM, Leckebusch GC, Pinto JG, Renggli D, Ulbrich S, Ulbrich U (2010) Cyclones causing wind storms in the Mediterranean: characteristics, trends and links to large-scale patterns. Nat Hazards Earth Syst Sci 10:1379–1391. doi:10.5194/nhess-10-1379-2010

Pinto JG, Spangehl T, Ulbrich U, Speth P (2005) Sensitivities of a cyclone detection and tracking algorithm: individual tracks and climatology. Meteor Z 14:823–838. doi:10.1127/0941-2948/2005/0068

Pinto JG, Spangehl T, Ulbrich U, Speth P (2006) Assessment of winter cyclone activity in a transient ECHAM4-OPYC3 GHG experiment. Meteor Z 15:279–291. doi:10.1127/0941-2948/2006/0128

Pinto JG, Ulbrich U, Leckebusch GC, Spangehl T, Reyers M, Zacharias S (2007) Changes in storm track and cyclone activity in three SRES ensemble experiments with the ECHAM5/MPI-OM1 GCM. Clim Dyn 29:195–210. doi:10.1007/s00382-007-0230-4

Pinto JG, Zacharias S, Fink AH, Leckebusch GC, Ulbrich U (2009) Factors contributing to the development of extreme North Atlantic cyclones and their relationship with the NAO. Clim Dyn 32:711–737. doi:10.1007/s00382-008-0396-4

Pinto JG, Karremann MK, Born K, Della-Marta PM, Klawa M (2012) Loss potentials associated with European windstorms under future climate conditions. Clim Res 54:1–20. doi:10.3354/cr01111

Prezerakos NG, Flocas HA, Michaelides SC (1999) Upper-tropospheric downstream development leading to surface cyclogenesis in the central Mediterranean. Meteorol Appl 6:313–322. doi:10.1017/S1350482799001218

Raible CC, Ziv B, Saaroni H, Wild M (2010) Winter synoptic-scale variability over the Mediterranean Basin under future climate conditions as simulated by the ECHAM5. Clim Dyn 35:473–488. doi:10.1007/s00382-009-0678-5

Roeckner E, Brokopf R, Esch M, Giorgetta M, Hagemann S, Kornblueh L, Manzini E, Schlese U, Schulzweida U (2006) Sensitivity of simulated climate to horizontal and vertical resolution in the ECHAM5 atmosphere model. J Clim 19:3771–3791. doi:10.1175/JCLI3824.1

Scoccimarro E, Gualdi S, Bellucci A, Sanna A, Fogli PG, Manzini E, Vichi M, Oddo P, Navarra A (2011) Effects of tropical cyclones on ocean heat transport in a high-resolution coupled general circulation model. J Clim 24:4368–4384. doi:10.1175/2011JCLI4104.1

Simmonds I, Murray RJ, Leighton RM (1999) A refinement of cyclone tracking methods with data from FROST. Aust Meteorol Mag Spec Ed, pp 35–49

Trigo IF (2006) Climatology and interannual variability of storm-tracks in the Euro-Atlantic sector: a comparison between ERA-40 and NCEP/NCAR reanalyses. Clim Dyn 26:127–143. doi:10.1007/s00382-005-0065-9

Trigo IF, Davies TD, Bigg GR (2000) Decline in Mediterranean rainfall caused by weakening of Mediterranean cyclones. Geophys Res Lett 27:2913–2916. doi:10.1029/2000GL011526

Ulbrich U, Leckebusch GC, Pinto JG (2009) Extra-tropical cyclones in the present and future climate: a review. Theor Appl Climatol 96:117–131. doi:10.1007/s00704-008-0083-8

Uppala SM, Kållberg PW, Simmons AJ, Andrae U, DaCosta Bechtold V, Fiorino M, Gibson JK, Haseler J, Hernandez A, Kelly GA, Li X, Onogi K, Saarinen S, Sokka N, Allan RP, Andersson E, Arpe K, Balmaseda MA, Beljaars ACM, VanDe Berg L, Bidlot J, Bormann N, Caires S, Chevallier F, Dethof A, Dragosavac M, Fisher M, Fuentes M, Hagemann S, Hólm E, Hoskins BJ, Isaksen L, Janssen PAEM, Jenne R, Mcnally AP, Mahfouf JF, Morcrette JJ, Rayner NA, Saunders RW, Simon P, Sterl A, Trenberth KE, Untch A, Vasiljevic D, Viterbo P, Woollen J (2005) The ERA40 reanalysis. Quart J Roy Meteorol Soc 131:2961–3012. doi:10.1256/qj.04.176